Geophysical Research Letters

RESEARCH LETTER
10.1029/2023GL104952

Multi-Temporal InSAR, GNSS and Seismic Measurements Reveal the Origin of the 2021 Vulcano Island (Italy) Unrest

F. Di Traglia[1,2], V. Bruno[3], F. Casu[2,4], O. Cocina[3], C. De Luca[2], F. Giudicepietro[1,2], G. Macedonio[1,2], M. Mattia[3], F. Monterroso[2], E. Privitera[3], and R. Lanari[2,4]

[1]Istituto Nazionale di Geofisica e Vulcanologia, Osservatorio Vesuviano, Napoli, Italy, [2]Consiglio Nazionale delle Ricerche, Istituto per il Rilevamento Elettromagnetico dell'Ambiente, Napoli-Milano, Italy, [3]Istituto Nazionale di Geofisica e Vulcanologia, Osservatorio Etneo, Catania, Italy, [4]Centro Nazionale "High Performance Computing, Big Data and Quantum Computing", Bologna, Italy

Abstract La Fossa Caldera at Vulcano (Italy) has been showing signs of unrest since September 2021. To investigate this phenomenon, we conducted an analysis of geodetic and seismological data from July to December 2021. In particular, we analyzed Multi Temporal Interferometric Synthetic Aperture Radar and Global Navigation Satellite System data, showing a pronounced elliptical uplift signal, which we elaborated using analytical source modeling. Additionally, seismic data were used to identify seismicity associated with hydrothermal system activity and assess its temporal evolution. The results indicate that the observed deformation is consistent with the expansion of the hydrothermal system within the La Fossa Caldera. These findings align with the analysis of seismic data, revealing signals indicative of hydrothermal activity, such as Very Long Period events. The results suggest that the ongoing phenomenon since 2021 represents a hydrothermal unrest, similar to the one observed during the late 1970s to early 1990s.

Plain Language Summary La Fossa Caldera at Vulcano Island, part of the Aeolian Islands archipelago in Italy, has shown an increased volcanic activity since September 2021. This activity is characterized by an increase in fumarole temperatures, massive gas emissions, as well as a marked uplift of the crater area, accompanied by an increase in seismicity. To investigate the nature of these phenomena, an analysis of ground deformation data obtained from Multi Temporal Interferometric Synthetic Aperture Radar and Global Navigation Satellite System measurements is presented. Additionally, a detailed analysis of data recorded by the seismic network on Vulcano Island has been conducted. The results indicate that these anomalies can be attributed to the expansion of the hydrothermal system, a phenomenon previously observed in the late 1970s and early 1990s.

Key Points:

- Multi Temporal Interferometric Synthetic Aperture Radar enabled investigating localized ground deformation in the La Fossa Caldera
- The analysis of local seismicity indicates it is associated with the injection of fluids into conduit-like structures
- The modeled source of ground deformation associated with the 2021 unrest is consistent with the pressurization of the hydrothermal system

Supporting Information:

Supporting Information may be found in the online version of this article.

Correspondence to:

V. Bruno,
valentina.bruno@ingv.it

Citation:

Di Traglia, F., Bruno, V., Casu, F., Cocina, O., De Luca, C., Giudicepietro, F., et al. (2023). Multi-temporal InSAR, GNSS and seismic measurements reveal the origin of the 2021 Vulcano Island (Italy) unrest. *Geophysical Research Letters*, *50*, e2023GL104952. https://doi.org/10.1029/2023GL104952

Received 14 JUN 2023
Accepted 16 NOV 2023

Author Contributions:

Conceptualization: F. Di Traglia, V. Bruno, F. Casu, O. Cocina, C. De Luca, F. Giudicepietro, G. Macedonio, M. Mattia, E. Privitera, R. Lanari
Data curation: F. Di Traglia, V. Bruno, F. Casu, C. De Luca, F. Giudicepietro, G. Macedonio, F. Monterroso, R. Lanari
Formal analysis: F. Di Traglia, V. Bruno, F. Casu, C. De Luca, F. Giudicepietro, G. Macedonio, F. Monterroso, R. Lanari
Funding acquisition: F. Casu, C. De Luca, F. Giudicepietro, R. Lanari

1. Introduction

This study analyzes the geodetic and seismic signals associated with the ongoing unrest in La Fossa Caldera, located in the northern part of Vulcano Island (Italy) within the Aeolian volcanic arc (Figures 1a and 1b). The unrest began in September 2021 and is still ongoing (September 2023; Aiuppa et al., 2022; Federico et al., 2023; Inguaggiato et al., 2022). Vulcano, along with Lipari, forms a volcanic ridge oriented NNW–SSE along the regional Aeolian-Tindari-Letojanni Fault (ATLF; Figure 1c) system (Barberi et al., 1994; Barreca et al., 2014; Mattia et al., 2008). The formation of La Fossa Caldera occurred between 55ky and 21ky, followed by volcanic activity in various vents within and on the caldera rim (La Fossa cone, Vulcanello, Faraglione; Selva et al., 2020). After the last Vulcanian eruption (1888–1890; Mercalli & Silvestri, 1891), intense and fluctuating hydrothermal activity have characterized Vulcano (Granieri et al., 2006; Montalto, 1996), often associated with ground deformation, as observed in 1985–1990 (inflation; Alparone et al., 2019) and 1990–1996 (deflation of a vertical, elongated, ellipsoidal depressurized source situated beneath the La Fossa cone at sea level; Gambino & Guglielmino, 2008). Local seismicity primarily occurs within the first few kilometers below the caldera floor, and it includes Long Period (LP) and Tornillos events, related to hydrothermal activity (Alparone et al., 2010, 2019; Cannata et al., 2012; Del Pezzo & Martini, 1981; Montalto, 1994).

Since September 2021, Vulcano has undergone a new phase of unrest. Fumarolic activity increased in the latter half of September, accompanied by intensified seismic activity (Coppola et al., 2022; Corradino et al., 2023; Federico et al., 2023; Inguaggiato et al., 2023). Notably, Very Long Period (VLP; frequency peak ~ 0.3 Hz)

Investigation: F. Di Traglia, V. Bruno, F. Casu, O. Cocina, C. De Luca, F. Giudicepietro, G. Macedonio, M. Mattia, F. Monterroso, E. Privitera, R. Lanari
Methodology: F. Di Traglia, V. Bruno, F. Casu, O. Cocina, C. De Luca, F. Giudicepietro, G. Macedonio, M. Mattia, F. Monterroso, E. Privitera, R. Lanari
Project Administration: F. Giudicepietro, R. Lanari
Resources: M. Mattia, R. Lanari
Software: G. Macedonio
Supervision: F. Di Traglia, R. Lanari
Validation: F. Di Traglia, V. Bruno, F. Casu, O. Cocina, C. De Luca, F. Giudicepietro, G. Macedonio, M. Mattia, E. Privitera, R. Lanari
Visualization: F. Di Traglia, V. Bruno, F. Casu, C. De Luca, G. Macedonio, F. Monterroso
Writing – original draft: F. Di Traglia, V. Bruno, F. Casu, O. Cocina, C. De Luca, F. Giudicepietro, G. Macedonio, M. Mattia, F. Monterroso, E. Privitera, R. Lanari
Writing – review & editing: F. Di Traglia, V. Bruno, F. Casu, O. Cocina, F. Giudicepietro, G. Macedonio, M. Mattia

seismic events were recorded for the first time, with the source area located at 950 ± 270 m below sea level, North of La Fossa cone (Federico et al., 2023). VLP events were attributed to fluid release within La Fossa Caldera's fracture network, and the source's consistent location suggests a connection between pressurized fluids and geological structures (Di Giuseppe et al., 2023; Federico et al., 2023).

Volcano Tectonic (VT) seismicity was at low levels before and during the mid-September unrest phase, with foci mainly located offshore to the W and SW of the island at intermediate depths (5–12 km). After 30 October 2021, there was a moderate increase in seismic activity in the NW and N sectors offshore of Vulcanello. Shallow seismicity persisted until December 2021. Subsequently, the seismic activity shifted to intermediate depths, with epicenters both on the island and offshore to the East (Federico et al., 2023).

In this work, ground deformation detected by using Multi-Temporal Interferometric Synthetic Aperture Radar (MT-InSAR) and Global Navigation Satellite System (GNSS) network (Figure 1c) data, were analyzed to identify the source of deformation, whereas the seismic network (Figure 1c) data were mainly exploited to characterize the seismicity induced by the hydrothermal system activity.

2. Materials and Methods

2.1. InSAR Data Processing

The Parallel Small BAseline Subset, P-SBAS (Casu et al., 2014; Manunta et al., 2019) technique was used to generate ground displacement time-series and velocity maps of Vulcano Island, with accuracies of about 5–10 mm and 1–2 mm/year, respectively. We used the P-SBAS algorithm to examine the entire C-band Sentinel-1 (S-1) data archive acquired from both ascending (Track 44) and descending (Track 124) orbits, covering the period March 2015 to September 2022. Here, we focus on the July–December 2021 period, when the S-1 constellation consisted of two identical satellites, enabling us to achieve a revisit time of as little as 6 days. Interferograms have been generated at the full spatial resolution of the sensor, by using a SRTM DEM to compensate for the topographic phase component and finally averaged (multilooked) to reach a pixel size of about 15 by 15 m. The accurate S-1 synchronization and the small orbital tube make the interferometric phase less sensitive to possible orbit and topography related errors, allowing us to only consider temporal constraints on the interferometric pairs selection. Moreover, the atmospheric phase screen (APS) has been filtered out from the displacement time series by first removing the signal which is highly correlated with topography but poorly in time, and then by filtering the residual APS component estimated from the non-deforming pixels (De Luca et al., 2022).

2.2. GNSS Network and Data Processing

The GNSS network is made up of 6 permanent stations (5 in Vulcano and 1 in Lipari. Figure 1c). GNSS data were processed using the GAMIT/GLOBK software (Herring et al., 2015, 2018) with IGS precise satellite orbits. Data from 12 IGS (International GNSS Service) stations (BOR1, GLSV, GRAS, GRAZ, LROC, MATE, NOT1, POTS, VILL, WSRT, WTZR, ZIMM) and a GNSS station (EIIV), installed in Catania (eastern Sicily) by the INGV, were also included in the processing. The GAMIT module was employed to derive loosely constrained daily solutions, providing coordinates and parameter estimates for each station along with their respective covariance matrices. By using the GLORG module of GLOBK, the loosely constrained daily solutions were translated and rotated to align them with the Eurasian reference frame (Altamimi et al., 2016). The final product of the GAMIT/GLOBK analyses is a three-component time series of daily station positions with respect to the Eurasian fixed reference frame. We used an elevation-dependent weighting for the phase data. The outliers were removed, the white noise was estimated for each station through the Hector software (Bos et al., 2013) and included in the error model used for the time series.

2.3. Seismic Network and Data Processing

The INGV OE seismic network installed at Vulcano and Lipari consists of 15 stations (Figure 1c), 9 of which were installed soon after the beginning of the unrest phase. All are equipped with broadband three-component velocimetric sensors and 5 of them with accelerometers. Data acquired in the remote stations are continuously transmitted to the operation room in Catania by way of different transmission methods (satellite, Wi-Fi, UMTS). Here, we focused on relevant seismic signals relevant for the hydrothermal system activity and transport of fluids

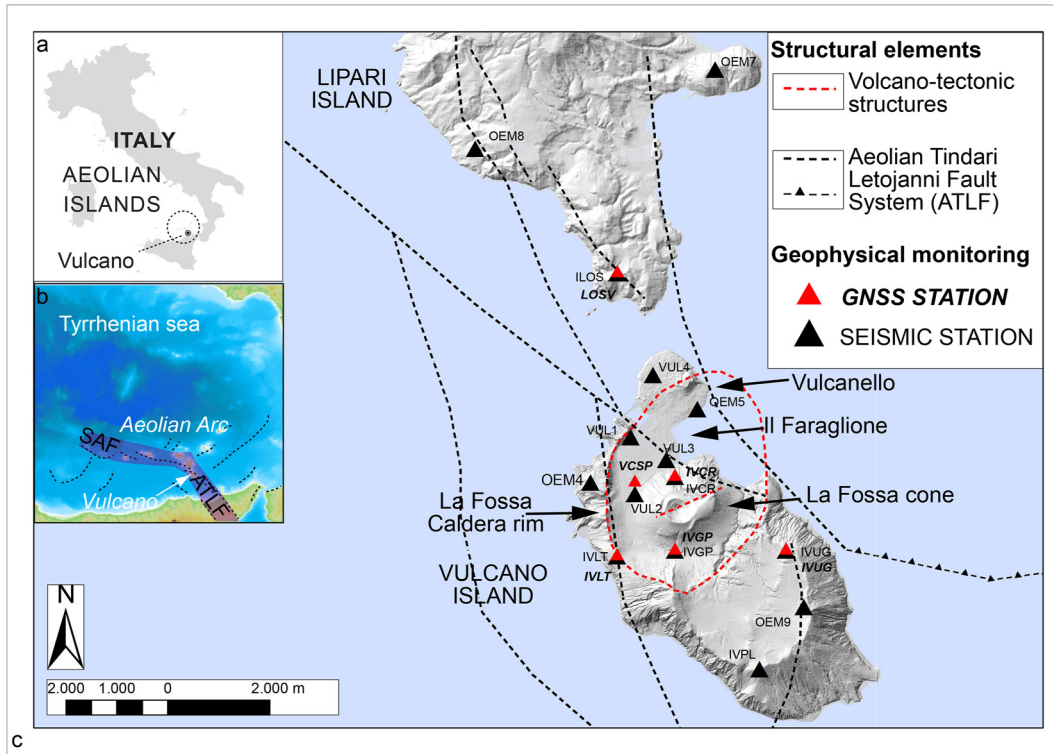

Figure 1. (a) and (b) Location of the study area. (c) Structural setting of Vulcano and Lipari, including regional tectonics (Aeolian Tindari Letojanni Fault - ATLF and Sisifo Alicudi Fault - SAF systems). The distribution of the GNSS and seismic networks installed on Vulcano is also reported.

through conduits, such as VLP events (Chouet & Matoza, 2013). VLPs are generally attributed to fluids passing through magma or hydrothermal conduits. In their study, Federico et al. (2023) employed a method based on radial semblance, similar to previous research on Etna and Stromboli (Cannata et al., 2012; Martini et al., 2007), to determine the affected zone of certain events. In our work, we expanded the analysis of seismic signals beyond just VLP occurrence rates, also considering VLP amplitude. This approach builds upon the method introduced by Giudicepietro et al. (2020) for defining the VLP size parameter in seismic signals associated with Stromboli explosions (Calvari et al., 2021; Di Traglia et al., 2014), a highly sensitive parameter to volcanoes' degassing processes (Giudicepietro et al., 2022). We analyzed the period from 1 July to 31 December 2021. We filtered the signal of the vertical component of the IVCR station in the 0.1–0.8 Hz band, around the peak frequency (0.3 Hz) of the Vulcano VLP events. We then split the signal for the entire period into two-minute windows. After applying the filter, we defined a 20-second sliding window, which moves over each two-minute window of signal with a 1-second shift. For each two-minute window of signal containing a VLP event we take the maximum value of the RSAM among the 100 ($120 - 20 = 100$) 20-second duration windows. We expressed the seismic amplitude as Real-time Seismic-Amplitude Measurement (RSAM), which is based on the average of the absolute value of the amplitude of a signal window (in our case length = 20 s), as defined by Endo and Murray (1991). To highlight the contribution in the seismic amplitude of only the data segments containing a VLP event, we set the seismic amplitude obtained for all data segments not containing any VLP event equal to 0. Thus, we obtained a time series with a time step of 2 min that represents the variation of the occurrence and the amplitude of VLP events well and that provides indications on the level of activity of the hydrothermal system.

2.4. Ground-Deformation Modeling

Analytical models are crucial for understanding how the crust responds to physical phenomena, helping us characterize driving mechanisms and determine source attributes such as location, size, orientation, and magnitude. To simulate ground deformation within the targeted volcanic region, we utilized models established by McTigue (1987) for a spherical source, Yang et al. (1988) for an inclined prolate spheroid, and Fialko et al. (2001)

for the inflation of a penny-shaped crack, all within a flat, elastic, homogeneous, isotropic half-space (refer to the Supporting Information S1). Although real volcanic sources are complex and not simple cavities with uniform shapes, we suggest that these models can provide a reasonable approximation of the strain field produced by actual reservoirs and transport pathways. In these models the volume change of the source ΔV is proportional to the ratio of the pressure variation ΔP and the shear modulus (rigidity) of the rock μ. The proportionality factor k depends on the geometry, the depth of the source and the Poisson's ratio ν:

$$\frac{\Delta P}{\mu} = k(\nu)\Delta V \tag{1}$$

In our work, we express the deformation in terms of the volume change of the source ΔV using Equation 1. The advantage of this approach is that the deformation does not depend on the rigidity μ, and only the dimensionless Poisson's ratio ν is needed for the inversion. Once the volume change ΔV is found, an estimate of the pressure increase can be acquired by using the same equation. Considering that the La Fossa Caldera infillings consist of lavas, hyaloclastites, and volcaniclastics (Gioncada & Sbrana, 1991) that have undergone significant hydrothermal alteration, particularly in the advanced argillitic alteration facies rich in clays (Fulignati et al., 1998), we selected a Geological Strength Index (GSI; Marinos & Hoek, 2000; Vásárhelyi, 2009; Hoek & Brown, 2019; Heap et al., 2020) range of 20–55 (as per Kereszturi et al., 2021). Based on laboratory-derived estimates of ν for volcanic rocks (Heap et al., 2009, 2014) and an empirical correlation between GSI and Poisson's ratio proposed by Heap et al., 2020, the corresponding ν falls within the range of 0.30–0.37. Ultimately, we opted for a value of $\nu = 0.35$, which we consider the most realistic choice for the rocks affected by the hydrothermal system at Vulcano. The results of a parametric study conducted on the various elastic models used for matching the ground deformation, also considering Poisson's ratio ν varying between 0.25 and 0.45, are detailed in Supporting Information S1 (Tables S1–S3).

We primarily used InSAR data for inversion analysis due to the lack of other geodetic measurements at the La Fossa cone's summit, which underwent the most significant deformation in the region (see Figure 2). In this confined area, InSAR data were used for effective monitoring of pronounced deformation. To validate measurement consistency, GNSS data were employed in areas with less intense deformation. Figures S5–S9 in Supporting Information S1 depict the comparison between deformation components derived from InSAR data and measurements from five GNSS stations. The inversion analysis considered cumulative displacement over the July-December 2021 period (see Figure 3). We assessed the results using the chi-square test and also incorporated time-varying ground deformation by considering the variable ΔV over time (see Figure 4). We assumed that the mechanical equilibrium's time scale is much shorter than that of pressure variations. The position of the center of the source has been considered constant over the period of time considered, whereas the strength of the source (ΔV) is allowed to vary with time. Concerning the potential impact of topography on model performance, it is worth noting that in the La Fossa Caldera, significant positive or negative relief features are not present. The maximum variation in topography is ≈300 m, with slopes <30° in areas of maximum deformation (Di Traglia et al., 2013). Consequently, it is anticipated that a flat model would provide sufficient accuracy for this region, as previously demonstrated for the Rabaul Caldera by Ronchin et al. (2015).

3. Results

Ground deformation data from July to December 2021 (Figure 2) showed rapid uplift compared to long-term displacements (see Figures S1 and S2 in Supporting Information S1 for MT-InSAR S-1 measurements from April 2015 to September 2022). InSAR-detected localized ground deformation mainly occurs within La Fossa Caldera, peaking at about 7 cm between January and late October 2021 along the ascending orbit, primarily within La Fossa cone crater (see Figure 2). The GNSS station IVCR, located on the northern flank of La Fossa cone, underwent the most significant displacement, while no GNSS data is available for the crater region. A comparison of InSAR and GNSS deformation data shows a good agreement (see Figure 2). The standard deviations of the discrepancies between InSAR data and GNSS time series, projected along the S-1 line of sight (LOS), have standard deviations less than 0.5 cm for both ascending and descending orbits.

The best-fitted source that we obtained by using InSAR data corresponds to the inflation of a dipping prolate spheroid (Yang et al., 1988), located at a depth of 598 m b.s.l. below La Fossa cone, with a geometric slope from the cone toward the center of the caldera (Figures 3 and 4). The prolate spheroid model provides the most realistic

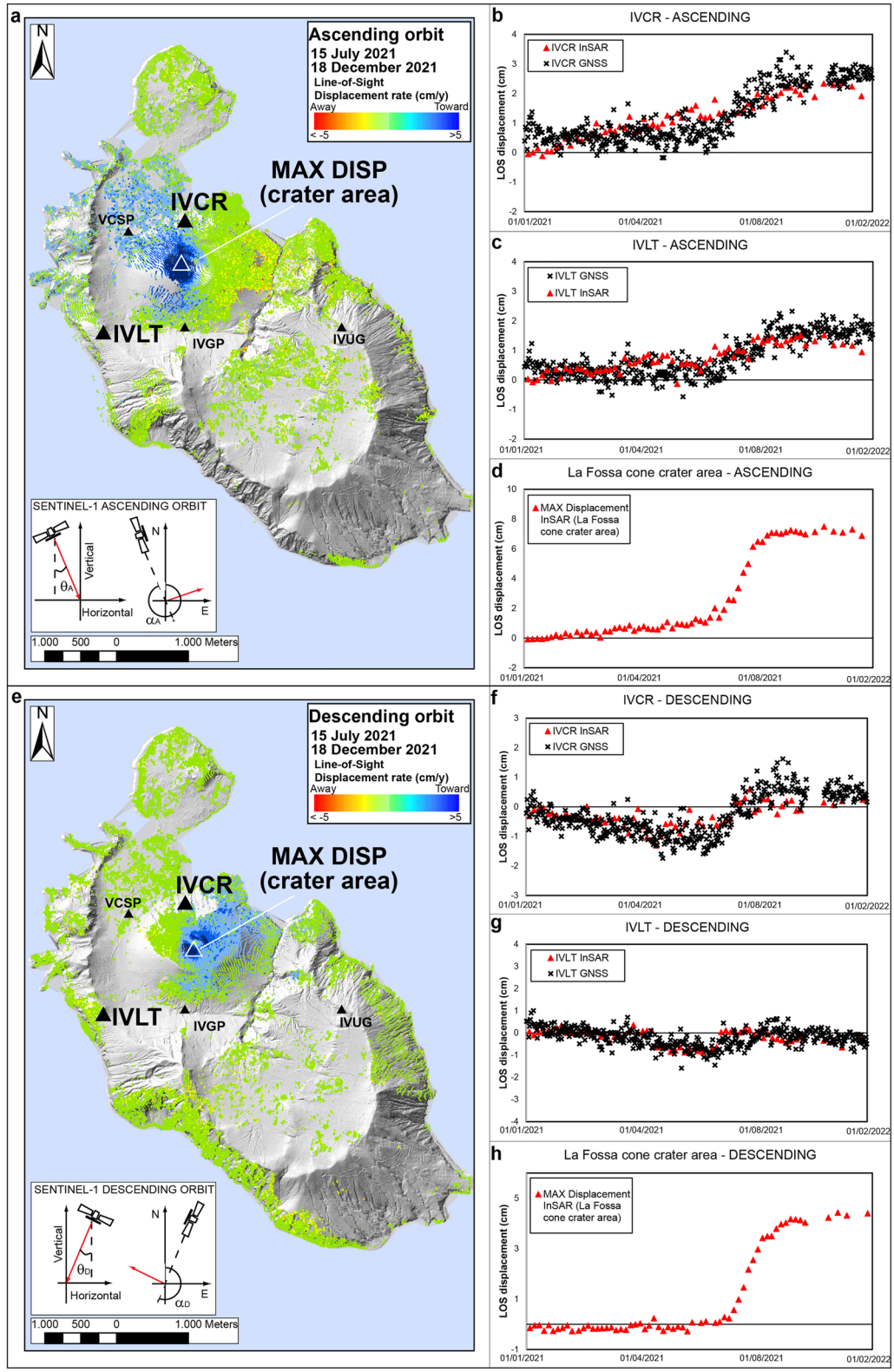

Figure 2. Ground deformation data from MT-InSAR and GNSS. Ascending (a) and descending (d) S-1 displacement rate maps (15 July–18 December 2021). Ascending (b, c) and descending (f, g) InSAR displacement time series in LOS, in the vicinity of the IVCR and IVLT stations (1 January 2021–1 February 2022). Ascending (d) and descending (h) time series of maximum InSAR displacement detected in the La Fossa cone crater area. Long-term deformation maps and time-series are reported in Supporting Information S1.

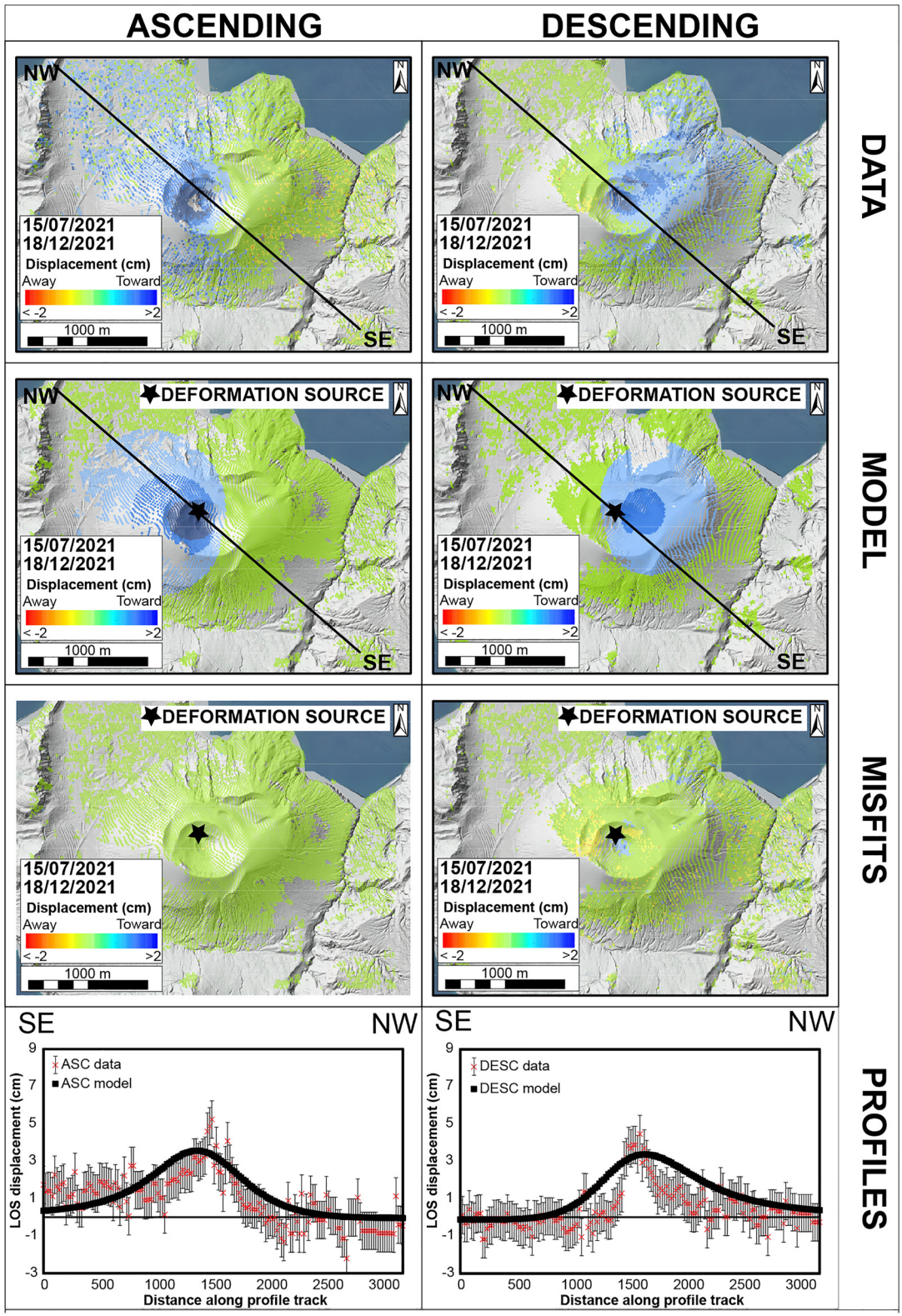

Figure 3. Cumulative ground displacement data, modeling results, residual maps (misfits), and deformation profiles, for both ascending and descending orbit, in the period 15 July–18 December 2021. The cumulative ground displacement was computed by differentiating the average of the last 3 and first 3 SAR epochs of the considered time interval. The error bar in the displacement data along the profiles is equal to 2σ of the measurements ($\sigma = 0.5$ cm). Most of the misfit between data and model are associated with the La Fossa cone fumarolic field.

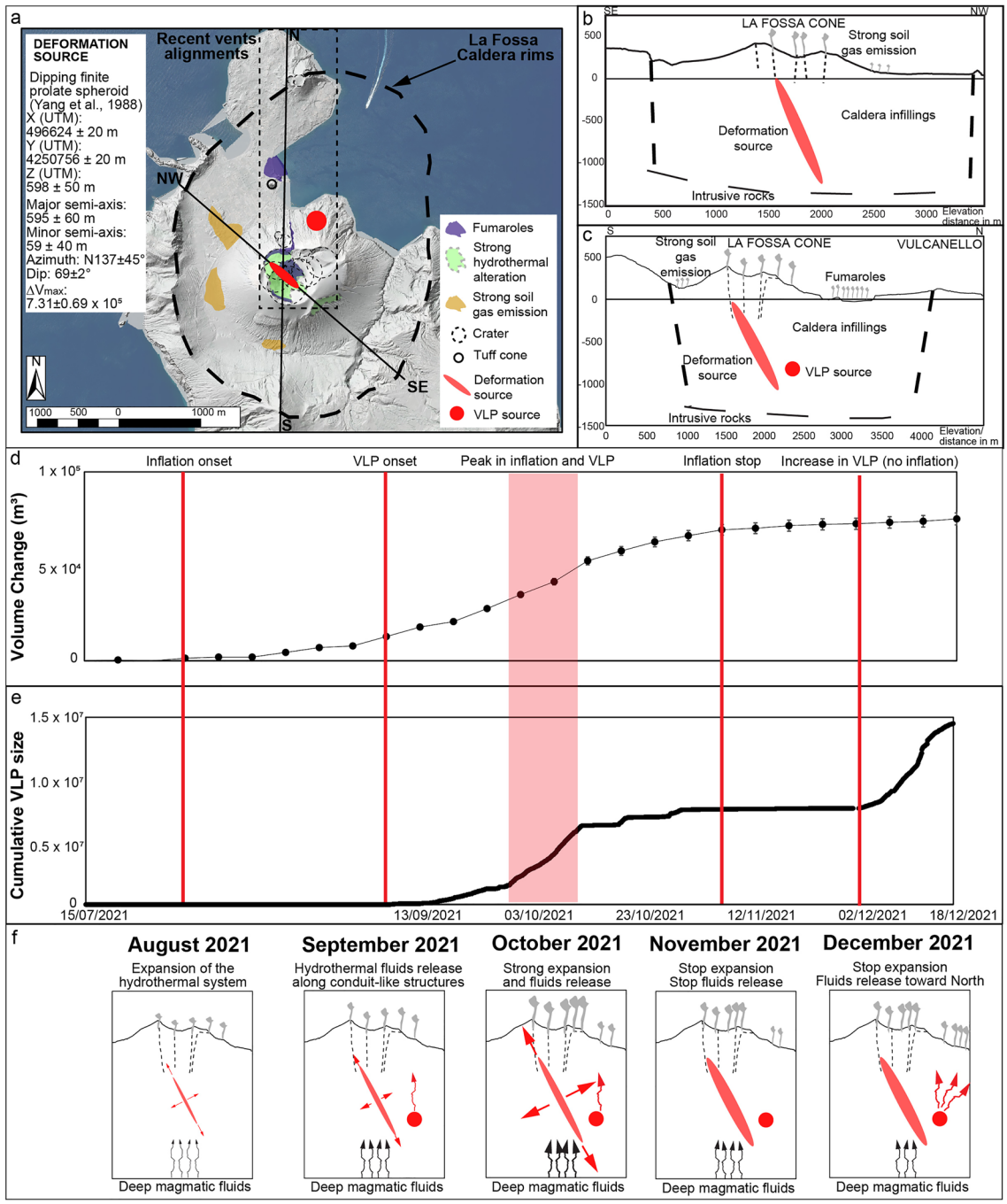

Figure 4. (a) La Fossa Caldera (from Romagnoli et al., 2012) with location of the deformation source (this study). The location of the VLPs and of the degassing areas, both diffuse and from fumarolic fields (Federico et al., 2023), the alignment of the recent vents of Vulcano and Lipari (Ruch et al., 2016) and the location of the summit craters of La Fossa cone (Di Traglia et al., 2013) are also reported. NW-SE profiles and N-S are included. (b) NW-SE and (c) N-S profiles showing the geometric relationship between the deformation source, that of the VLPs and the main structures of the La Fossa Caldera. In (d) and in (e) the time series of the source volume (from modeling geodetic data) and of the cumulative VLP size, respectively, are reported. The main phases of the initiation of unrest are also indicated. In (f) the interpretation of the observed phenomena is schematically reported, which foresee: (i) initial expansion phase of the hydrothermal system due to thermal and volatile input from deeper magmatic storage (3–5 km, Aiuppa et al., 2022) (August 2021); (ii) release of volatiles from the expanding hydrothermal system (onset of VLPs) and increased fumarolic activity (September 2021); (iii) climax of this unrest phase (October 2021); (iv) calm phase observed in November 2021, marked by the cessation of inflation and a temporary reduction in VLPs; (v) intense fluid release phase, accompanied by a significant number and amplitude of VLP signals, without concurrent hydrothermal system expansion (December 2021).

pressure values (3–8 MPa) for the source volume, while the other two models yield significantly higher pressures, exceeding the rock strength by one to three orders of magnitude (Tommasi et al., 2019), that is, a phreatic explosion would have occurred (Rosi et al., 2018). For these reasons we considered the prolate spheroid the most suitable model to represent the source of the detected deformation. The total volume change is $7.31 \pm 0.69 \times 10^5$ m^3 (reduced $\chi^2 = 0.23$; see Supporting Information S1), and the maximum $\Delta P = 8.48$ MPa.

The results of the seismological data analysis show that the cumulative amplitude of the VLP events shows a rapid increase when the rate of deformation and source pressure are higher (Figures 4d and 4e). This suggests a link between hydrothermal seismicity and the deformation source.

4. Discussion and Conclusions

The overall results presented here indicate that the investigated unrest phase (September-December 2021), that is, inflation and seismicity, together with anomalies in gasses emissions (Aiuppa et al., 2022; Federico et al., 2023; Inguaggiato et al., 2022, 2023), is compatible with the expansion of the hydrothermal system located within the La Fossa Caldera. Thermal anomalies also show a similar trend, with a peak again in October 2021 (Coppola et al., 2022; Corradino et al., 2023; Pailot-Bonnétat et al., 2023). While the thermal anomalies have been interpreted as an increase in temperatures of the fumarolic field present in the crater area of the La Fossa cone, the geochemical anomalies are interpreted as an increase in the parameters of the hydrothermal system which in turn is enriched in a strong and deep input of fluids released from an underlying magma batch (Aiuppa et al., 2022; Inguaggiato et al., 2022).

The prolate spheroid resulting from our inversion, with a major-to-minor axis ratio of approximately 10, is oriented in the NW-SE direction, aligning with the fractures that control the localization of fumaroles within the crater area of La Fossa cone (Barde-Cabusson et al., 2009; Mueller et al., 2021; Schopa et al., 2011). The source's position and configuration closely align with the La Fossa Caldera hydrothermal system, as described by Gioncada and Sbrana (1991), Fulignati et al. (1998), and Chiarabba et al. (2004). Di Giuseppe et al. (2023) have identified a conduit-like structure saturated with magma-derived fluids in good agreement with our modeled source. This finding is consistent with the interpretation of an elongated rock volume that facilitates the upward movement of fluids to the surface (Montanaro et al., 2020). Upon examining the comparison between detected and modeled data in Figure 3, it is evident that there is a better fit of the data in the ascending orbit compared to the descending orbit. This discrepancy may stem from local factors, including variations in the physical properties of the hydrothermalized material, which exhibits a highly irregular spatial distribution (Mueller et al., 2021; Schopa et al., 2011), or the presence of extremely localized deformation sources attributable to the surface fumarolic system (Bonaccorso et al., 2010; Revil et al., 2008).

The good agreement between the temporal evolution of the deformation source pressure and the appearance of the VLP events, in the period in which the deformation rate is maximum, suggests the link of the unrest with the increase in the activity of the hydrothermal system, the VLP seismicity being incontrovertibly associated with the passage of fluids in geological structures.

We further note that our results allow us to identify the temporal evolution of the occurred phenomena, which can be summarized as follows (Figure 4f):

- the La Fossa Caldera hydrothermal system went under pressure between late July and early September 2021;
- from 5 September 2021 (when the first VLP was recorded) to early November 2021, the pressurization of the hydrothermal system increases (peak reached in mid-October 2021);
- the occurrence of VLP, suggesting the gas transfer from the hydrothermal system, is coherent with the arrival of hydrothermal fluids at the surface (Federico et al., 2023);
- the alignment between the location of the VLP source and the fumarole areas inside the caldera (La Fossa cone, Faraglione) suggests the role of an N-S structure in the transfer of hydrothermal fluids (Bonaccorso et al., 2010; Di Giuseppe et al., 2023; Fulignati et al., 1998; Ruch et al., 2016);
- from the beginning of November onwards, the deformation does not increase, while a series of phenomena coherent with the northward shift begin to occur (increase of gas flux in the fumarolic field between the Faraglione and Vulcanello; Federico et al., 2023).

Localized deformation at volcanoes, such as those measured at La Fossa Caldera between early August and late October 2021, may be very relevant because they are often indicators of the hydrothermal systems pressurization and can be precursors of phreatic explosions (Bemelmans et al., 2023; Kobayashi et al., 2018). Accordingly, the combined use of MT-InSAR and GNSS data is valuable because it allows examining surface deformation and the time evolution of localized hydrothermal systems, along with the analysis of seismic signals. Additionally, the study highlights that in active volcanic regions, the elastic properties of rocks surrounding shallow hydrothermal systems can differ from unaltered rocks. This underscores the need for future in-depth investigations into altered volcanic materials to better understand their elastic behavior.

Data Availability Statement

The data reported in this paper are available in Di Traglia et al. (2023) and Istituto Nazionale di Geofisica e Vulcanologia (2005).

Acknowledgments

This study has been partly funded by the Italian DPC, in the frame of INGV-DPC (2022–2025) and IREA-DPC (2022–2024) agreements. This paper does not necessarily represent DPC official opinion and policies. We also acknowledge the support of EPOS-RI, including the one obtained through the EPOS-Italia JRU. This work benefited also from the Progetto ORME, INGV Project "Pianeta Dinamico" - Working Earth (CUP 1466 D53J19000170001 - legge 145/2018) (Scientific Responsibility: F.G.). The authors express their gratitude to Thomas Walter and an anonymous reviewer for their comments and suggestions, and to the editor Christian Huber for overseeing the article. This research was also partially funded by the European Union - NextGeneratonEU through the following projects: NRRP - MEET (National Recovery and Resilience Plan - Monitoring Earth's Evolution and Tectonics), ICSC - CN-HPC - PNRR M4C2 Investimento 1.4 - CN00000013, GeoSciences IR - PNRR M4C2 Investimento 3.1 - IR0000037.

References

Aiuppa, A., Bitetto, M., Calabrese, S., Delle Donne, D., Lages, J., La Monica, F. P., et al. (2022). Mafic magma feeds degassing unrest at Vulcano Island, Italy. *Communications Earth & Environment*, *3*(1), 255. https://doi.org/10.1038/s43247-022-00589-1

Alparone, S., Bonforte, A., Gambino, S., Guglielmino, F., Obrizzo, F., & Velardita, R. (2019). Dynamics of Vulcano Island (Tyrrhenian Sea, Italy) investigated by long-term (40 years) geophysical data. *Earth-Science Reviews*, *190*, 521–535. https://doi.org/10.1016/j.earscirev.2019.01.002

Alparone, S., Cannata, A., Gambino, S., Gresta, S., Milluzzo, V., & Montalto, P. (2010). Time-space variation of volcano-seismic events at La Fossa (Vulcano, Aeolian Islands, Italy): New insights into seismic sources in a hydrothermal system. *Bulletin of Volcanology*, *72*(7), 803–816. https://doi.org/10.1007/s00445-010-0367-6

Altamimi, Z., Rebischung, P., Métivier, L., & Collilieux, X. (2016). ITRF2014: A new release of the international Terrestrial reference Frame modeling nonlinear station motions. *Journal of Geophysical Research: Solid Earth*, *121*(8), 6109–6131. https://doi.org/10.1002/2016JB013098

Barberi, F., Gandino, A., Gioncada, A., La Torre, P., Sbrana, A., & Zenucchini, C. (1994). The deep structure of the Eolian arc (Filicudi-Panarea-Vulcano sector) in light of gravity, magnetic and volcanological data. *Journal of Volcanology and Geothermal Research*, *61*(3–4), 189–206. https://doi.org/10.1016/0377-0273(94)90003-5

Barde-Cabusson, S., Finizola, A., Revil, A., Ricci, T., Piscitelli, S., Rizzo, E., et al. (2009). New geological insights and structural control on fluid circulation in La Fossa cone (Vulcano, Aeolian Islands, Italy). *Journal of Volcanology and Geothermal Research*, *185*(3), 231–245. https://doi.org/10.1016/j.jvolgeores.2009.06.002

Barreca, G., Bruno, V., Cultrera, F., Mattia, M., Monaco, C., & Scarfì, L. (2014). New insights in the geodynamics of the Lipari-Vulcano area (Aeolian Archipelago, southern Italy) from geological, geodetic and seismological data. *Journal of Geodynamics*, *82*, 150–167. https://doi.org/10.1016/j.jog.2014.07.003

Bemelmans, M. J., Biggs, J., Poland, M., Wookey, J., Ebmeier, S. K., Diefenbach, A. K., & Syahbana, D. (2023). High-resolution InSAR reveals localized pre-eruptive deformation inside the crater of Agung volcano, Indonesia. *Journal of Geophysical Research: Solid Earth*, *128*(5), e2022JB025669. https://doi.org/10.1029/2022jb025669

Bonaccorso, A., Bonforte, A., & Gambino, S. (2010). Thermal expansion-contraction and slope instability of a fumarole field inferred from geodetic measurements at Vulcano. *Bulletin of Volcanology*, *72*(7), 791–801. https://doi.org/10.1007/s00445-010-0366-7

Bos, M. S., Fernandes, R. M. S., Williams, S. D. P., & Bastos, L. (2013). Fast error analysis of continuous GNSS observations with missing data. *Journal of Geodesy*, *87*(4), 351–360. https://doi.org/10.1007/s00190-012-0605-0

Calvari, S., Giudicepietro, F., Di Traglia, F., Bonaccorso, A., Macedonio, G., & Casagli, N. (2021). Variable magnitude and intensity of Strombolian explosions: Focus on the eruptive processes for a first classification scheme for Stromboli volcano (Italy). *Remote Sensing*, *13*(5), 944. https://doi.org/10.3390/rs13050944

Cannata, A., Diliberto, I. S., Alparone, S., Gambino, S., Gresta, S., Liotta, M., et al. (2012). Multiparametric approach in investigating volcano-hydrothermal systems: The case study of Vulcano (Aeolian Islands, Italy). *Pure and Applied Geophysics*, *169*(1–2), 167–182. https://doi.org/10.1007/s00024-011-0297-z

Casu, F., Elefante, E., Imperatore, P., Zinno, I., Manunta, M., De Luca, C., & Lanari, R. (2014). SBAS-DInSAR parallel processing for deformation time series computation. *IEEE JSTARS*, *7*(8), 3285–3296. https://doi.org/10.1109/JSTARS.2014.2322671

Chiarabba, C., Pino, N. A., Ventura, G., & Vilardo, G. (2004). Structural features of the shallow plumbing system of Vulcano Island Italy. *Bulletin of Volcanology*, *66*(6), 477–484. https://doi.org/10.1007/s00445-003-0331-9

Chouet, B. A., & Matoza, R. S. (2013). A multi-decadal view of seismic methods for detecting precursors of magma movement and eruption. *Journal of Volcanology and Geothermal Research*, *252*, 108–175. https://doi.org/10.1016/j.jvolgeores.2012.11.013

Coppola, D., Laiolo, M., Campus, A., & Massimetti, F. (2022). Thermal unrest of a fumarolic field tracked using VIIRS imaging bands: The case of La fossa crater (Vulcano Island, Italy). *Frontiers in Earth Science*, *10*, 1534. https://doi.org/10.3389/feart.2022.964372

Corradino, C., Ramsey, M. S., Pailot-Bonnétat, S., Harris, A. J., & Del Negro, C. (2023). Detection of subtle thermal anomalies: Deep learning applied to the ASTER global volcano dataset. *IEEE Transactions on Geoscience and Remote Sensing*, *61*, 1–15. https://doi.org/10.1109/tgrs.2023.3241085

Del Pezzo, E., & Martini, M. (1981). Seismic events under Vulcano, Aeolian Islands, Italy. *Bulletin Volcanologique*, *44*(3), 521–525. https://doi.org/10.1007/bf02600583

De Luca, C., Valerio, E., Giudicepietro, F., Macedonio, G., Casu, F., & Lanari, R. (2022). Pre- and co-eruptive analysis of the september 2021 eruption at Cumbre Vieja Volcano (La Palma, Canary Islands) through DInSAR measurements and analytical modeling. *Geophysical Research Letters*, *49*(7), e2021GL097293. https://doi.org/10.1029/2021GL097293

Di Giuseppe, M. G., Isaia, R., & Troiano, A. (2023). Three-dimensional magnetotelluric modeling of Vulcano Island (Eolie, Italy) and its implications for understanding recent volcanic unrest. *Scientific Reports*, *13*(1), 16458. https://doi.org/10.1038/s41598-023-43828-x

Di Traglia, F., Bruno, V., Casu, F., Cocina, O., De Luca, C., Giudicepietro, F., et al. (2023). Multi-temporal InSAR, GNSS and seismic measurements reveal the origin of the 2021 Vulcano Island (Italy) unrest [Dataset]. FIGSHARE. https://doi.org/10.6084/m9.figshare.23501664

Di Traglia, F., Cauchie, L., Casagli, N., & Saccorotti, G. (2014). Decrypting geophysical signals at Stromboli Volcano (Italy): Integration of seismic and ground-based InSAR displacement data. *Geophysical Research Letters*, *41*(8), 2753–2761. https://doi.org/10.1002/2014gl059824

Di Traglia, F., Pistolesi, M., Rosi, M., Bonadonna, C., Fusillo, R., & Roverato, M. (2013). Growth and erosion: The volcanic geology and morphological evolution of La Fossa (Island of Vulcano, Southern Italy) in the last 1000 years. *Geomorphology*, *194*, 94–107. https://doi.org/10.1016/j.geomorph.2013.04.018

Endo, E. T., & Murray, T. (1991). Real-time seismic amplitude measurement (RSAM): A volcano monitoring and prediction tool. *Bulletin of Volcanology*, *53*(7), 533–545. https://doi.org/10.1007/bf00298154

Federico, C., Cocina, O., Gambino, S., Paonita, A., Branca, S., Coltelli, M., et al. (2023). Inferences on the 2021 ongoing Volcanic unrest at Vulcano Island (Italy) through a comprehensive multidisciplinary surveillance network. *Remote Sensing*, *15*(5), 1405. https://doi.org/10.3390/rs15051405

Fialko, Y., Khazan, Y., & Simons, M. (2001). Deformation due to a pressurized horizontal circular crack in an elastic half-space, with applications to volcano geodesy. *Geophysical Journal International*, *146*(1), 181–190. https://doi.org/10.1046/j.1365-246x.2001.00452.x

Fulignati, P., Gioncada, A., & Sbrana, A. (1998). Geologic model of the magmatic hydrothermal system of vulcano (Aeolian Islands, Italy). *Mineralogy and Petrology*, *62*(3–4), 195–222. https://doi.org/10.1007/bf01178029

Gambino, S., & Guglielmino, F. (2008). Ground deformation induced by geothermal processes: A model for La Fossa Crater (Vulcano Island, Italy). *Journal of Geophysical Research*, *113*(B7), B07402. https://doi.org/10.1029/2007jb005016

Gioncada, A., & Sbrana, A. (1991). La Fossa Caldera, Vulcano: Inferences from deep drillings. *Acta Vulcanologica*, *1*, 115–125.

Giudicepietro, F., Calvari, S., D'Auria, L., Di Traglia, F., Layer, L., Macedonio, G., et al. (2022). Changes in the eruptive style of Stromboli volcano before the 2019 paroxysmal phase discovered through SOM clustering of seismo-acoustic features compared with camera images and GBInSAR data. *Remote Sensing*, *14*(5), 1287. https://doi.org/10.3390/rs14051287

Giudicepietro, F., López, C., Macedonio, G., Alparone, S., Bianco, F., Calvari, S., et al. (2020). Geophysical precursors of the July-August 2019 paroxysmal eruptive phase and their implications for Stromboli volcano (Italy) monitoring. *Scientific Reports*, *10*(1), 1–16. https://doi.org/10.1038/s41598-020-67220-1

Granieri, D., Carapezza, M. L., Chiodini, G., Avino, R., Caliro, S., Ranaldi, M., et al. (2006). Correlated increase in CO_2 fumarolic content and diffuse emission from La Fossa crater (Vulcano, Italy): Evidence of volcanic unrest or increasing gas release from a stationary deep magma body? *Geophysical Research Letters*, *33*(13), L13316. https://doi.org/10.1029/2006gl026460

Heap, M. J., Villeneuve, M., Albino, F., Farquharson, J. I., Brothelande, E., Amelung, F., et al. (2020). Towards more realistic values of elastic moduli for volcano modelling. *Journal of Volcanology and Geothermal Research*, *390*, 106684. https://doi.org/10.1016/j.jvolgeores.2019.106684

Heap, M. J., Vinciguerra, S., & Meredith, P. G. (2009). The evolution of elastic moduli with increasing crack damage during cyclic stressing of a basalt from Mt. Etna volcano. *Tectonophysics*, *471*(1–2), 153–160. https://doi.org/10.1016/j.tecto.2008.10.004

Heap, M. J., Xu, T., & Chen, C. F. (2014). The influence of porosity and vesicle size on the brittle strength of volcanic rocks and magma. *Bulletin of Volcanology*, *76*(9), 1–15. https://doi.org/10.1007/s00445-014-0856-0

Herring, T. A., King, R., Floyd, M. A., & McClusky, S. C. (2018). GAMIT reference manual: GPS analysis at MIT, release 10.7; department of earth. Tech. Rep.

Herring, T. A., King, R. W., Floyd, M. A., & McClusky, S. C. (2015). GLOBK: Global Kalman filter VLBI and GPS analysis program. *Reference manual*.

Hoek, E., & Brown, E. T. (2019). The Hoek–Brown failure criterion and GSI–2018 edition. *Zealand Journal of Geology and Geophysics*, *64*(2–3), 421–442.

Inguaggiato, S., Liotta, M., Rouwet, D., Tassi, F., Vita, F., Schiavo, B., et al. (2023). Sulfur origin and flux variations in fumarolic fluids of Vulcano Island, Italy. *Frontiers in Earth Science*, *11*. https://doi.org/10.3389/feart.2023.1197796

Inguaggiato, S., Vita, F., Diliberto, I. S., Inguaggiato, C., Mazot, A., Cangemi, M., & Corrao, M. (2022). The volcanic activity changes occurred in the 2021–2022 at Vulcano island (Italy), inferred by the abrupt variations of soil CO2 output. *Scientific Reports*, *12*(1), 21166. https://doi.org/10.1038/s41598-022-25435-4

Istituto Nazionale di Geofisica e Vulcanologia (INGV) (2005). Rete Sismica Nazionale (RSN). Istituto Nazionale di Geofisica e Vulcanologia (INGV) [Dataset]. EIDA. https://doi.org/10.13127/SD/X0FXNH7QFY

Kereszturi, G., Schaefer, L., Mead, S., Miller, C., Procter, J., & Kennedy, B. (2021). Synthesis of hydrothermal alteration, rock mechanics and geophysical mapping to constrain failure and debris avalanche hazards at Mt. Ruapehu (New Zealand). *New Zealand Journal of Geology and Geophysics*, *64*(2–3), 421–442.

Kobayashi, T., Morishita, Y., & Munekane, H. (2018). First detection of precursory ground inflation of a small phreatic eruption by InSAR. *Earth and Planetary Science Letters*, *491*, 244–254. https://doi.org/10.1016/j.epsl.2018.03.041

Manunta, M., De Luca, C., Zinno, I., Casu, F., Manzo, M., Bonano, M., et al. (2019). The parallel SBAS approach for Sentinel-1 interferometric wide swath deformation time-series generation: Algorithm description and products quality assessment. *IEEE Transactions on Geoscience and Remote Sensing*, *57*(9), 6259–6281. https://doi.org/10.1109/tgrs.2019.2904912

Marinos, P., & Hoek, E. (2000). GSI: A geologically friendly tool for rock mass strength estimation. In *ISRM international symposium*. OnePetro.

Martini, M., Giudicepietro, F., D'Auria, L., Esposito, A. M., Caputo, T., Curciotti, R., et al. (2007). Seismological monitoring of the February 2007 effusive eruption of the Stromboli volcano. *Annals of Geophysics*, *50*(6).

Mattia, M., Palano, M., Bruno, V., Cannavo, F., Bonaccorso, A., & Gresta, S. (2008). Tectonic features of the Lipari–Vulcano complex (Aeolian archipelago, Italy) from 10 years (1996–2006) of GPS data. *Terra Nova*, *20*(5), 370–377. https://doi.org/10.1111/j.1365-3121.2008.00830.x

McTigue, D. F. (1987). Elastic stress and deformation near a finite spherical magma body: Resolution of the point source paradox. *Journal of Geophysical Research*, *92*(B12), 12931–12940. https://doi.org/10.1029/jb092ib12p12931

Mercalli, G., & Silvestri, O. (1891). Le eruzioni dell'Isola di Vulcano incominciate il 3 agosto 1888 e terminate il 22 marzo 1890, relazione scientifica. *Ann Ufficio Centrale Metereol Geodin Ital*, *10*, 1–213.

Montalto, A. (1994). Seismic signals in geothermal areas of active volcanism: A case study from 'La Fossa', Vulcano (Italy). *Bulletin of Volcanology*, *56*(3), 220–227. https://doi.org/10.1007/bf00279607

Montalto, A. (1996). Signs of potential renewal of eruptive activity at La Fossa (Vulcano, Aeolian Islands). *Bulletin of Volcanology*, *57*(7), 483–492. https://doi.org/10.1007/bf00304434

Montanaro, C., Cronin, S., Scheu, B., Kennedy, B., & Scott, B. (2020). Complex crater fields formed by steam-driven eruptions: Lake Okaro, New Zealand. *GSA Bulletin*, *132*(9–10), 1914–1930. https://doi.org/10.1130/b35276.1

Müller, D., Bredemeyer, S., Zorn, E., De Paolo, E., & Walter, T. R. (2021). Surveying fumarole sites and hydrothermal alteration by unoccupied aircraft systems (UAS) at the La Fossa cone, Vulcano Island (Italy). *Journal of Volcanology and Geothermal Research*, *413*, 107208. https://doi.org/10.1016/j.jvolgeores.2021.107208

Pailot-Bonnétat, S., Rafflin, V., Harris, A., Diliberto, I. S., Ganci, G., Cappello, A., et al. (2023). Anatomy of thermal unrest at a hydrothermal system: Case study of the 2021-2022 crisis at Vulcano.PREPRINT (Version 1) available at Research Square. https://doi.org/10.21203/rs.3.rs-2911239/v1

Revil, A., Finizola, A., Piscitelli, S., Rizzo, E., Ricci, T., Crespy, A., et al. (2008). Inner structure of La Fossa di Vulcano (Vulcano Island, southern Tyrrhenian Sea, Italy) revealed by high-resolution electric resistivity tomography coupled with self-potential, temperature, and CO_2 diffuse degassing measurements. *Journal of Geophysical Research*, *113*(B7), B07207. https://doi.org/10.1029/2007jb005394

Romagnoli, C., Casalbore, D., & Chiocci, F. L. (2012). La Fossa Caldera breaching and submarine erosion (Vulcano island, Italy). *Marine Geology*, *303*, 87–98. https://doi.org/10.1016/j.margeo.2012.02.004

Ronchin, E., Geyer, A., & Martí, J. (2015). Evaluating topographic effects on ground deformation: Insights from finite element modeling. *Surveys in Geophysics*, *36*(4), 513–548. https://doi.org/10.1007/s10712-015-9325-3

Rosi, M., Di Traglia, F., Pistolesi, M., Esposti Ongaro, T., de'Michieli Vitturi, M., & Bonadonna, C. (2018). Dynamics of shallow hydrothermal eruptions: New insights from Vulcano's Breccia di Commenda eruption. *Bulletin of Volcanology*, *80*(12), 1–28. https://doi.org/10.1007/s00445-018-1252-y

Ruch, J., Vezzoli, L., De Rosa, R., Di Lorenzo, R., & Acocella, V. (2016). Magmatic control along a strike-slip volcanic arc: The central Aeolian arc (Italy). *Tectonics*, *35*(2), 407–424. https://doi.org/10.1002/2015tc004060

Schopa, A., Pantaleo, M., & Walter, T. R. (2011). Scale-dependent location of hydrothermal vents: Stress field models and infrared field observations on the Fossa Cone, Vulcano Island, Italy. *Journal of Volcanology and Geothermal Research*, *203*(3–4), 133–145. https://doi.org/10.1016/j.jvolgeores.2011.03.008

Selva, J., Bonadonna, C., Branca, S., De Astis, G., Gambino, S., Paonita, A., et al. (2020). Multiple hazards and paths to eruptions: A review of the volcanic system of Vulcano (Aeolian Islands, Italy). *Earth-Science Reviews*, *207*, 103186. https://doi.org/10.1016/j.earscirev.2020.103186

Tommasi, P., Graziani, A., Rotonda, T., & Bevivino, C. (2019). Preliminary analysis of instability phenomena at Vulcano Island, Italy. Taylor & Francis Group.

Vásárhelyi, B. (2009). A possible method for estimating the Poisson's rate values of the rock masses. *Acta Geodaetica et Geophysica Hungarica*, *44*(3), 313–322. https://doi.org/10.1556/ageod.44.2009.3.4

Yang, X. M., Davis, P. M., & Dieterich, J. H. (1988). Deformation from inflation of a dipping finite prolate spheroid in an elastic half-space as a model for volcanic stressing. *Journal of Geophysical Research*, *93*(B5), 4249–4257. https://doi.org/10.1029/jb093ib05p04249